



Phosphate Removal from Synthetic Stormwater Using Chitosan and Clay

Gaurav Verma¹; Jagadeesh Kumar Janga²; Krishna R. Reddy³; and Angelica M. Palomino⁴

Abstract: Excessive levels of phosphate in stormwater runoff can negatively impact receiving surface water bodies, such as retention ponds, and may also seep into groundwater. Liner systems composed of materials with greater phosphate selectivity have the potential to mitigate infiltration and eliminate phosphate. One potential material is chitosan, an abundant naturally occurring biopolymer. This study evaluated five materials for their ability to remove phosphate from synthetic stormwater using batch tests with different initial phosphate concentrations ranging from 0.5 to 12 mg/L and a fixed 24-h exposure time. The materials included two types of clayey soils (kaolin and bentonite) and three different varieties of chitosan with varying molecular weights (low, medium, and high). The phosphate removal efficiency of kaolin was found to be the highest, with efficiencies ranging from 100% to 56% at different concentrations, while bentonite was found to be the least effective, with removal efficiencies ranging from 40% to 12%. The removal efficiencies of all three types of chitosans analyzed were higher than those of bentonite but lower than those of kaolin. The removal efficiencies ranged from 77% to 19% for low-molecularweight chitosan, 84% to 31% for medium-molecular-weight chitosan, and 55% to 18% for high-molecular-weight chitosan. The removal mechanism of phosphate by kaolin and bentonite was attributed to surface adsorption and precipitation. In chitosan, the likely mechanism is electrostatic attraction. The maximum adsorption capacity for kaolin was not reached under the tested phosphate concentration range, indicating potential adsorption sites remained available on the particle surfaces. The results for bentonite, low-molecular-weight chitosan, and high-molecular-weight chitosan showed that these materials nearly reached their maximum adsorption capacities, indicating that fewer adsorption sites were remaining. The Langmuir adsorption isotherm was found to be the best-fit model for phosphate adsorption in all the materials tested compared to the Freundlich isotherm. According to the Langmuir model, the maximum adsorption capacities for kaolin, bentonite, low-molecular-weight chitosan, medium-molecular-weight chitosan, and high-molecular-weight chitosan were found to be 140.85, 33, 48.78, 82.64, and 51.28 mg/kg, respectively. DOI: 10.1061/JHTRBP.HZENG-1270. © 2023 American Society of Civil Engineers.

Author keywords: Adsorption; Phosphate; Stormwater runoff; Chitosan; Kaolin; Bentonite.

Introduction

Greenhouse gases, such as CO₂ and CH₄, are continuously introduced into the atmosphere through human and industrial activities, causing significant harm to the environment (USEPA 2022a). These gases are known to contribute to global warming, resulting in a rise in the Earth's temperature, which, if unchecked, could result in catastrophic consequences (USEPA 2022b). Global

¹Graduate Research Assistant, Dept. of Civil, Materials, and Environmental Engineering, Univ. of Illinois Chicago, 842 West Taylor St., Chicago, IL 60607. ORCID: https://orcid.org/0009-0000-2385-6088. Email: gverma5@uic.edu

²Graduate Research Assistant, Dept. of Civil, Materials, and Environmental Engineering, Univ. of Illinois Chicago, 842 West Taylor St., Chicago, IL 60607. ORCID: https://orcid.org/0000-0002-8293-5808. Email: jreddy3@uic.edu

³Professor, Dept. of Civil, Materials, and Environmental Engineering, Univ. of Illinois Chicago, 842 West Taylor St., Chicago, IL 60607 (corresponding author). ORCID: https://orcid.org/0000-0002-6577-1151. Email: kreddy@uic.edu

⁴Associate Professor, Dept. of Civil and Environmental Engineering, Univ. of Tennessee Knoxville, 423 John D. Tickle Building, Knoxville, TN 37996. ORCID: https://orcid.org/0000-0002-9999-6252. Email:apalomin@utk.edu

Note. This manuscript was submitted on April 19, 2023; approved on August 9, 2023; published online on September 21, 2023. Discussion period open until February 21, 2024; separate discussions must be submitted for individual papers. This paper is part of the *Journal of Hazardous*, *Toxic, and Radioactive Waste*, © ASCE, ISSN 2153-5493.

warming can alter the distribution, intensity, and frequency of rainfall. Some areas may experience increased precipitation, leading to heavier downpours and an increased risk of flooding. In contrast, other regions may face reduced rainfall, resulting in more frequent and severe droughts. Consequently, prioritizing the adoption of effective stormwater management strategies, such as stormwater retention ponds, can help prevent floods, replenish groundwater, and safeguard water quality. Urban areas are differentiated from rural areas by the extensive prevalence of impermeable surfaces, such as roads, sidewalks, pavements, and parking areas (Adhikari et al. 2016). The impermeable nature of these surfaces, constructed from materials such as concrete, asphalt, and stone, inhibits the infiltration of stormwater and leads to an increased volume of stormwater runoff (Deng 2020). Moreover, as stormwater flows across these impervious surfaces, pollutants from various sources, such as vehicles, fluid leaks, pesticides, fertilizers, and pet feces, are carried indiscriminately along with the flowing water. Contaminant types often include nutrients like phosphates, heavy metals, and hydrocarbons (Alam and Faisal Anwar 2020; Harmayani and Faisal Anwar 2016).

Phosphate is a limiting nutrient essential for plant growth, but if present in excessive amounts, eutrophication may occur in receiving surface waterbodies (rivers, lakes, and retention ponds). This may lead to the disturbance of the whole marine ecosystem (Ma et al. 2009). The concentration of phosphate in stormwater exhibits variations across different locations and storm events. Lee and Bang (2000) found that phosphate concentrations in stormwater runoff in Chongju City, South Korea varied from 0 to 8 mg/L,

depending on the type of watershed (industrial or residential). May and Sivakumar (2009) analyzed stormwater quality data from the United States and found that total phosphorous concentrations range from 0 to 1 mg/L for residential or agricultural land use. However, higher concentrations of 4-8 mg/L were reported when the dominant land use was for commercial or industrial purposes. In addition, infiltration of PO_4^{3-} -P-contaminated stormwater in retention ponds into the groundwater may contaminate the groundwater as well. One established method of mitigating the infiltration of contaminants into groundwater is using a liner system in retention ponds. The efficacy of such liner systems depends on the liner material composition. Clays are commonly employed as liner materials due to their low hydraulic conductivity (<10⁻⁹ m/s) (Deka and Sekharan 2017). Although this approach may reduce the infiltration of contaminated stormwater, it does not eliminate the contaminants from the stormwater. To fulfill both objectives of reducing infiltration and removing contaminants, the liner material must have low hydraulic conductivity and high adsorption properties for various contaminants present in stormwater and be readily available, replaceable, and cost-effective (Sharma and Reddy 2004). Research has demonstrated that clay composites augmented with materials such as fly ash can possess low hydraulic properties and effectively remove contaminants from the infiltrated liquid (Deka and Sekharan 2017). Such composites, employing low permeable materials in combination with waste materials or industrial byproducts, can serve as technically sound liner materials while also improving the sustainability of the liner system.

Chitosan—a natural biopolymer—has gained significant attention as a nonconventional sorbent due to its cost-effectiveness, wide availability, biocompatibility, biodegradability, nontoxicity, and high reactivity (Szymczyk et al. 2016; Eltaweil et al. 2021). Chitosan is produced by deacetylating chitin, a biopolymer found in the exoskeletons of crustaceans, fungi, and insects. Chitin is the second most abundant natural biopolymer after cellulose (Eltaweil et al. 2021). The removal of acetyl groups from chitin increases the number of active amino (-NH₂) groups, which serve as the primary adsorption sites for ions (Liu et al. 2022). Studies have demonstrated that chitosan is a viable adsorbent for diverse pollutants in the treatment of wastewater (Gamage and Shahidi 2007; Guibal et al. 2006; Miretzky and Cirelli 2009; Pontoni and Fabbricino 2012). This has led to a growing interest in exploring its potential application in geoenvironmental engineering, such as an amendment to remediate contaminated soils (Kamari et al. 2011) and as a coating for sand to remediate contaminated groundwater as a permeable reactive barrier (Wan et al. 2004). In addition, chitosan is generally regarded as nontoxic and safe to use. Chitosan has demonstrated a favorable toxicological profile, both as a food additive and in potable water treatment. Acute toxicity tests using organisms such as Oryzias latipes and Daphnia magna showed that chitosan-treated water and chitosan-based flocculants exhibit low toxicity levels (Yang et al. 2016). Thus, chitosan has the potential to be used as an effective, low-cost, and nontoxic material in clay composite liners due to its abundant availability and contaminant adsorption capabilities.

This study aimed to compare the effectiveness of chitosan and selected clayey soils in removing phosphate. Batch experiments were conducted on three types of chitosans with varying molecular weights (low, medium, and high) and two types of clay soils, kaolin and bentonite (Na-montmorillonite). These experiments were carried out to evaluate the efficacy of these materials in removing phosphate from synthetic stormwater of varying initial phosphate concentrations. The outcomes of the experiments were to determine the phosphate adsorption capacity of each material and evaluate

any potential impact of pH, oxidation-reduction potential (ORP), and electrical conductivity (EC) on the removal efficiency.

Materials and Methods

Materials

Five materials were selected for the adsorption batch studies: kaolin, bentonite, and low-, medium-, and high-molecular-weight chitosan. Kaolin, predominantly composed of kaolinite, is a naturally occurring aluminosilicate clay material, and it was obtained from Rio Grande do Sul state (Brazil). The bentonite used here consists mostly of montmorillonite and was obtained from Soledade, Para-iba (Brazil). The physical and chemical properties of kaolin and bentonite used in this study are presented in Tables 1 and 2, and the general chemical structures of kaolinite, montmorillonite, and chitosan are shown in Fig. 1. The chemical composition was determined previously using X-ray fluorescence spectrometry (XRF) (Ferrazzo et al. 2020). The analysis utilized the STD-1 calibration, which allows for nonstandard evaluation of chemical elements ranging from fluorine to uranium. The fluorescence spectrometer used was an S8 Tiger model, Bruker.

Chitosan is a substance obtained from the deacetylation of chitin, a linear mucopolysaccharide primarily found in the

Table 1. Physical properties of bentonite and kaolin

Property	Bentonite	Kaolin	Standard used
G_s (g/cm ³)	2.68	2.67	ASTM D854-14, ASTM 2014a
Liquid limit (%)	193	44	ASTM D4318, ASTM 2017
Plastic limit (%)	36	32	ASTM D4318, ASTM 2017
pH (water)	8.66	6.71	ASTM D4972-19, ASTM 2019
Particle size	_	_	ASTM D422, ASTM 2016
distribution (%)			
0.6-0.2 mm	_	0.2	_
0.2-0.06 mm	3.41	7	_
0.06-0.002 mm	46.17	58	_
< 0.002 mm (%)	50.42	35	_

Table 2. Chemical properties of bentonite and kaolin

Chemical composition (%) (XRF)	Bentonite	Kaolin
Na ₂ O	0.797	< 0.001
MgO	0.981	0.142
Al_2O_3	31.400	35.800
SiO_2	46.500	47.400
P_2O_5	00.051	0.020
SO_3	0.032	0.081
Cl	0.129	< 0.001
K ₂ O	1.240	0.845
CaO	1.170	0.111
TiO_2	0.358	0.154
V_2O_5	< 0.001	< 0.001
Cr_2O_3	0.013	< 0.001
MnO	0.012	0.014
Fe_2O_3	2.620	1.170
CuO	< 0.001	< 0.001
ZnO	< 0.001	< 0.001
As_2O_3	< 0.001	< 0.001
SrO	_	< 0.001
Y_2O_3	< 0.001	< 0.001
ZrO_2	0.018	< 0.001
BaO	0.046	0.053
CoO	< 0.001	< 0.001
Rb ₂ O	< 0.001	< 0.001

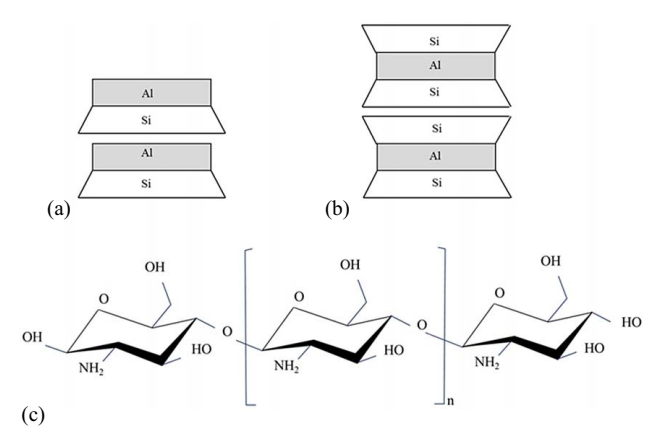


Fig. 1. General chemical structures of (a) kaolinite; (b) montmorillonite (adapted from Holtz et al. 2011); and (c) chitosan (adapted from Feng et al. 2021; Abd El-Hack et al. 2020). Si = silica tetrahedral sheet: and Al = alumina octahedral sheet.

exoskeletons of arthropods and some fungal cell walls. The degree of deacetylation, molecular weight, and source of feedstock are some key factors that can affect chitosan characteristics. During the process of deacetylation of chitin, the degree of deacetylation, which refers to the number of acetyl groups removed, increases with the duration of the deacetylation process. However, prolonged reaction times negatively impact the molecular weight of chitosan (Tolaimate et al. 2000). A decrease in molecular weight (fewer monomer units in a single polymer chain) reduces the number of active adsorption sites (Mirzai and Asadabadi 2022). Therefore, molecular weight is a factor in determining the phosphate adsorption capacity of chitosan. The source of feedstock for the low- and high-molecular-weight chitosan used in this study are shrimp shells, while a blend of crab and shrimp shells was used to derive the medium-molecular-weight chitosan. The physical properties of the selected chitosans, as provided by the vendor, are listed in Table 3. All three chitosan materials were purchased from a commercial source (Sigma-Aldrich), and the selected materials were used as-is without any modification.

Phosphate Solutions

The concentration of phosphate in stormwater runoff is known to vary widely across different locations and storm events. A typical

Table 3. Physical properties of chitosan

Property	Chitosan-low	Chitosan-medium	Chitosan-high	
Product no.	448869	448877	419419	
Appearance				
Color	Light beige	Offwhite to faint beige	Faint beige	
Form	Powder	Crystals	Powder	
Formula	$C_{12}H_{24}N_2O_9$	$C_{12}H_{24}N_2O_9$	$C_{12}H_{24}N_2O_9$	
Melting point (°C)	102.5	102.5	102.5	
Source	Shrimp shells	Mixed crab and shrimp	Shrimp shells	
		shells		
pН	_	_	6.5 - 8.0	
Molecular weight	50,000-	190,000-310,000	310,000-	
(Da)	190,000		375,000	
Viscosity (cps)	113	300-494	1,218-1,232	
Degree of	76	87–88	76	
deacetylation (%)				

Source: Ian Brockie (personal communication, June 12, 2023).

range of phosphate (PO_4^{3-} -P) concentration in stormwater varies between 0 and 8 mg/L depending on the type of watershed (Lee and Bang 2000; May and Sivakumar 2009; Li et al. 2012; Reddy et al. 2014). Hence, five different concentrations of PO_4^{3-} -P were selected for this study: 0.5, 1, 2, and 4 mg/L (low concentrations) and 12 mg/L (high concentration). Batch test solutions were prepared by first making a standard stock solution of 100 mg/L PO_4^{3-} -P using potassium dihydrogen phosphate (KI_2PO_4) and deionized water. The selected concentrations of phosphate (PO_4^{3-} -P) solution were obtained by diluting the standard stock solution based on the calculated dilution ratios.

Batch Experimental Procedures

Batch experiments were conducted in the laboratory to evaluate the removal efficiency of each clay/chitosan material under various initial PO₄³-P concentrations. The removal efficiency of contaminants is influenced by various factors, such as the initial concentration of the solution, contact time between the adsorbent and adsorbate, pH, and others. Experiments were performed at each PO₄³--P concentration with each clay/chitosan material to investigate the phosphate removal capability of the selected materials. To conduct the batch test, 1 g of each clay or chitosan material was added to a 50-mL centrifuge tube along with 20 mL of various PO₄³⁻-P solutions. Control suspensions made of 1 g of each clay or chitosan material and 20 mL of deionized water were also tested to determine whether any of the clay/chitosan materials leached phosphate. The tubes were then tightly capped and shaken in a tumbler for 24 h at room temperature, which was assumed to be the time required to reach equilibrium (OECD 2000; Hance 1967). After 24 h, the samples were centrifuged at 5,000 rpm for varying durations, depending on the material. The purpose of centrifugation was to separate the solids from the phosphate supernatant and to facilitate subsequent vacuum filtration. The supernatant solution was then filtered through a 0.45-µm filter membrane using a vacuum filtration system. The filtrate was then transferred and stored in 40-mL glass vials for further testing and analysis. The pH, ORP, and EC were analyzed for all the collected filtrates. The concentration of phosphate in all samples was analyzed using a UV-vis spectrophotometer at 400 nm wavelength. The mass of PO₄³-P adsorbed per unit dry mass of each clay or chitosan material was calculated by using the formula given as follows:

$$S = \frac{V(C_0 - C_e)}{M} \tag{1}$$

where C_o = initial PO₄³⁻-P concentration (mg/L); C_e = final PO₄³⁻-P concentration after 24 h (mg/L); V = volume of phosphate solution (mL); and M = mass of each material (g) added during the batch test. All tests were carried out in duplicate.

Analytical Procedures

The value of pH is a measure of the acidity or alkalinity of a solution and quantifies the concentration of hydrogen ions (H⁺) present in the solution. Several studies have demonstrated that a change in pH can affect the phosphate adsorption capacities of soils and chitosan composites (Zhou et al. 2005; Rajeswari et al. 2015). Additionally, the ORP, measured in millivolts (mV), is commonly used to assess the oxidation state of a chemical using Eh–pH plots, where Eh represents the measured ORP value in volts (V) (Sharma and Reddy 2004). Any change in pH and ORP may change the oxidation state of phosphate ions (Pasek 2008), which can in turn affect the adsorption reactions. EC indicates the number of free ions present in the filtrate solutions. Hence, the pH, ORP,

and EC of the test solutions were measured before and after each batch experiment. The pH and ORP of the filtrate samples collected at the end of the batch experiments were measured using the "Traceable pH/ORP Meter with Calibration" (ASTM D1293, ASTM 2018; D1498, ASTM 2014b). The electrical conductivity of the filtrate samples was measured using a "4366 Traceable Conductivity/TDS Pen" (ASTM D1125, ASTM 2023). Additionally, the pH, ORP, and EC of the prepared phosphate solutions, without clay/chitosan materials, were also measured. These measurements were made to better understand the adsorption mechanism of phosphate on each material at different concentrations.

The PO_4^{3-} -P concentrations in the filtrate samples taken at the end of the batch experiments were determined using the "4500-P C. Colorimetric Method of Vanadomolybdophosphoric Acid" (APHA, AWWA, WEF 2005). The method of determining phosphate in a solution involves the reaction of ammonium molybdate with phosphate in an acidic environment to form molybdophosphoric acid, which, in the presence of vanadium, forms vanadomolybdophosphoric acid, which is yellow in color. The more intense the yellow color, the higher the concentration of phosphate in a solution. Two solutions (A and B) were prepared. Solution A was made by adding 2.5 g of ammonium molybdate to 30 mL of deionized water (DI) water, while Solution B was prepared by dissolving 0.125 g of ammonium metavanadate in 30 mL of DI water and heating the mixture below the boiling point until complete dissolution occurs. After cooling, 33 mL of concentrated HCl (36.5%) was added to Solution B. Solution A was then mixed with the resulting Solution B and diluted to 100 mL with DI water. A calibration curve was plotted for phosphate analysis using the same concentrations selected for the batch experiments: PO_4^{3-} -P concentrations of 0, 0.5, 1, 2, 4, and 12 mg/L. For determining phosphate concentration in the filtrates, 4 mL of the filtrate sample was mixed with 1 mL of vanadate-molybdate reagent. The mixture was left at room temperature for 10 min to develop a stable yellow color, and the absorbance was recorded at a wavelength of 400 nm.

Adsorption Isotherms

An adsorption isotherm represents the relationship between the amounts of nutrients (phosphate) adsorbed onto a unit dry mass of the selected material and the concentration of these nutrients (phosphate) in the solution at equilibrium. This relationship was developed in the present study using both the Langmuir and Freundlich models. The Langmuir isotherm model was initially developed for solid—gas interactions but can also be applied to solid—liquid interactions (Kalam et al. 2021). This model assumes a homogeneous surface of the adsorbent, monolayer adsorption of the adsorbate onto the adsorbent, and a lack of lateral interactions between the adsorbed nutrients on the surface of the adsorbent (Kalam et al. 2021). The mathematical description of this model can be represented as follows:

$$S = \frac{\alpha \beta C}{1 + \alpha C} \tag{2}$$

where S= amount of nutrients (mg/g) per unit dry mass of material; and C= equilibrium concentration of the nutrients (mg/L). α (L/mg) and β (mg/kg) can be determined from the Langmuir isotherm, and C/S plotted is as a function of C. The slope of the line is $(1/\beta)$, and the y-intercept is $(1/\alpha\beta)$. The Freundlich isotherm model assumes multilayer adsorption on a heterogenous surface of an adsorbent (Kalam et al. 2021) and can be represented as

follows:

$$S = KC^N \tag{3}$$

where K (L/kg) and N can be determined from the isotherm by plotting S (on a log scale) as a function of C (on a log scale). The slope of the line is N, and log K is the y-intercept.

Results and Discussion

Filtrate Solution Properties

Fig. 2 shows the pH, ORP, and EC of solution samples for pure phosphate solutions (no clay or chitosan) and the postbatch experiment supernatant solutions obtained after filtration for each clay or chitosan material for the tested phosphate concentrations. Measurements of pH, ORP, and EC are each presented as the average of two values (duplicate tests). The solution properties of the initial phosphate solutions (without clay or chitosan) were observed to exhibit variations within the following ranges: pH, 6-7.2; ORP, 256-279 mV; and EC, 0-0.04 mS/cm. The solution properties for the kaolin batch tests ranged from 6.4 to 6.8 for pH, 244.40 to 279.15 mV for ORP, and 0.02 to 0.06 mS/cm for EC. Numerous studies have described the pH dependency of dissolution rates of kaolin minerals in suspensions. The resulting products of these dissolution reactions, in turn, have an impact on the pH of the suspension. When no catalysts are present, the dissolution of oxides and silicates in kaolin can be categorized into three mechanisms: proton-promoted, water-promoted, and hydroxyl-promoted. These mechanisms dominate the dissolution rate under acidic, neutral, and basic pH ranges. The dissolution reactions in the acidic, neutral, and basic pH ranges for kaolin, as reported in previous literature, are shown as follows (Cama and Ganor 2015):

$$Al_2Si_2O_5(OH)_4 + 6H^+ \rightarrow 2Al^{3+} + 2H_4SiO_4 + H_2O$$
 (4)

$$Al_2Si_2O_5(OH)_4 + 7H_2O \rightarrow 2AL(OH)_4^- + 2H_4SiO_4 + 2H^+$$
 (5)

$$Al_2Si_2O_5(OH)_4 + 5H_2O + 2OH^- \rightarrow 2AL(OH)_4^- + 2H_4SiO_4$$
 (6)

In the conducted batch experiments, no significant differences were observed in pH, ORP, or EC between the properties of the initial phosphate solutions (without added clay) and the postbatch experiment filtrate solution at the corresponding concentrations, as shown in Fig. 2. Furthermore, no noticeable trends were observed for pH, EC, or ORP with increasing phosphate concentration. The measured pH and EC values for all tested phosphate concentrations with kaolin fell within narrow ranges. Under the slightly acidic or neutral conditions of both DI and the phosphate solutions used in the experiment, as evident from Fig. 2(a), the dissolution of kaolin might lead to the generation of free Al³⁺ ions or (Al(OH)₄)⁻ ions [Eqs. (4), and (5)], which can potentially influence the pH, ORP, or EC of the filtrate solutions. However, no significant differences were observed in pH, ORP, or EC between the no-kaolin and kaolin filtrate solutions. Thus, the changes in these properties before and after the batch tests indicate that their influence on the adsorption or removal of phosphate by kaolin is insignificant.

The postbatch experiment solution properties for bentonite indicated significantly higher values of pH and EC and lower values of ORP compared to the corresponding phosphate solutions without clay or chitosan (Fig. 2). The measured supernatant solution properties at the end of the batch experiments for bentonite were pH = 9.6–9.9, ORP = 149.25–165 mV, and EC = 0.54–0.69 mS/cm. Results for the measurements of postbatch experiment solution

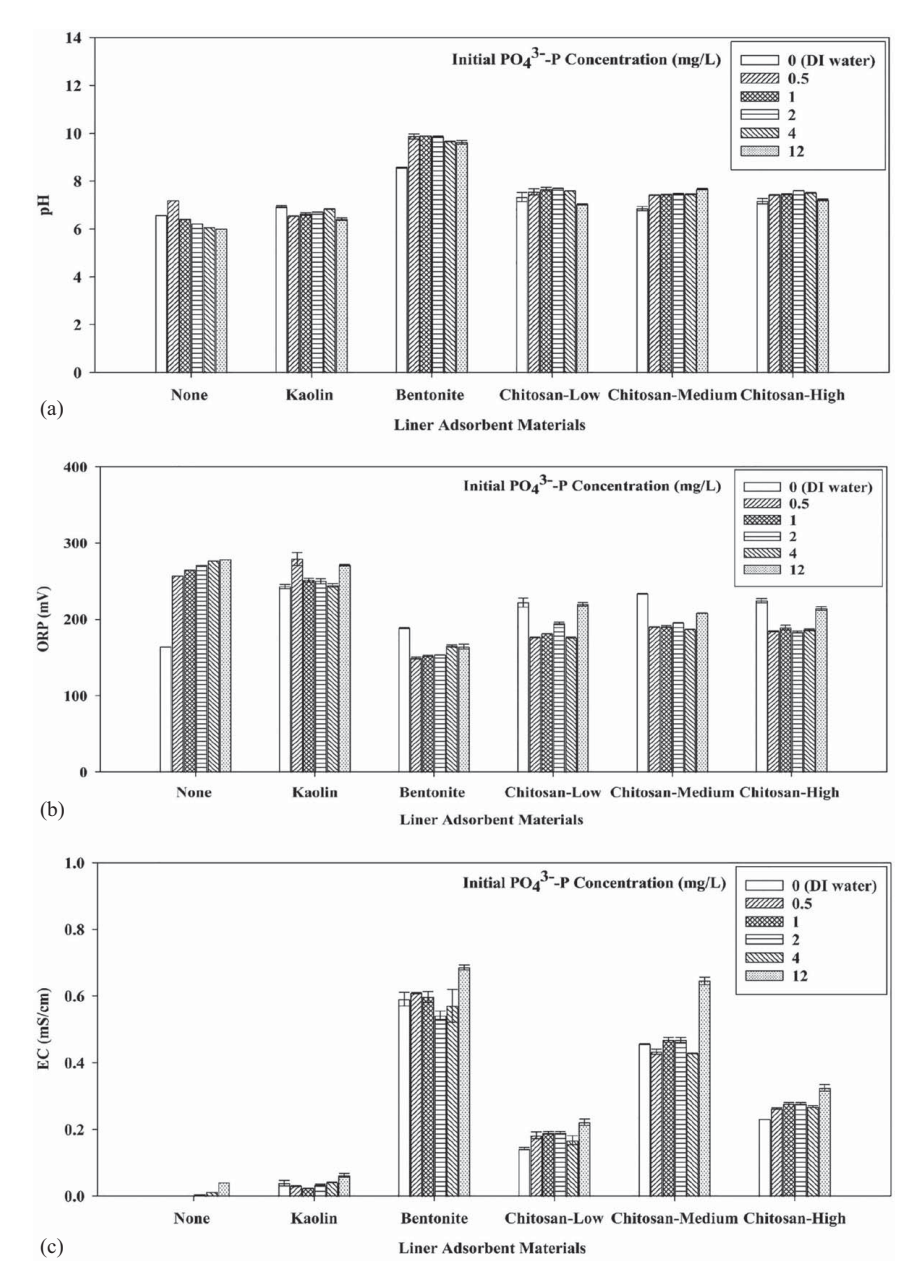


Fig. 2. Solution properties of deionized water, pure phosphate solutions (no exposure to clay or chitosan), and postbatch experiment solutions for the selected materials: (a) pH; (b) ORP; and (c) EC.

properties with bentonite indicated that the addition of phosphate led to an increase in pH and a decrease in ORP compared to the DI cases. The pH of the bentonite-DI water filtrate solution obtained after the batch experiment was also higher than that of pure deionized water (no bentonite). Previous studies have examined the reasons for the alkaline pH of Na-bentonite aqueous suspensions and factors affecting the same aforementioned potential mechanisms (Kaufhold et al. 2008). The main reasons attributed to the alkaline reaction of Na-montmorillonite with water are the hydrolysis of montmorillonite (exchange of Na⁺ ions from bentonite with H⁺ ions in water) and the increase in the volume of the stern layer due to delamination (binding H⁺ ions in the strongly held stern layer) (Kaufhold et al. 2008). Furthermore, the consistently higher pH observed for the phosphate solution for bentonite, compared to the deionized water cases [Fig. 2(a)] aligns with previous research findings. This effect may be attributed to the release of hydroxyls into the solution following the fixation of phosphate ions

onto the surface of bentonite (Yaghoobi-Rahni et al. 2017). For all cases with bentonite in phosphate solutions, narrow ranges of final pH and ORP were observed. EC values were also within a narrow range except for the case with an initial phosphate concentration of 12 mg/L, in which the EC was significantly greater than the other tested cases. In this case, for 12 mg/L initial phosphate concentration, as the removal efficiency observed was very low (approximately 12%), the higher observed EC is likely due to the higher number of free phosphate ions in the filtrate.

Solutions exposed to chitosan had slightly higher pH values, lower ORP values, and higher EC values compared to the corresponding phosphate solutions without chitosan or clay. Chitosan is known to be a weak base, resulting in a higher pH and lower ORP (Qin et al. 2006). No significant differences were observed in the measured pH values with increasing phosphate concentration for any of the tested chitosan materials, with pH values ranging from 7.0 to 7.7. No distinct relationship between ORP and increasing

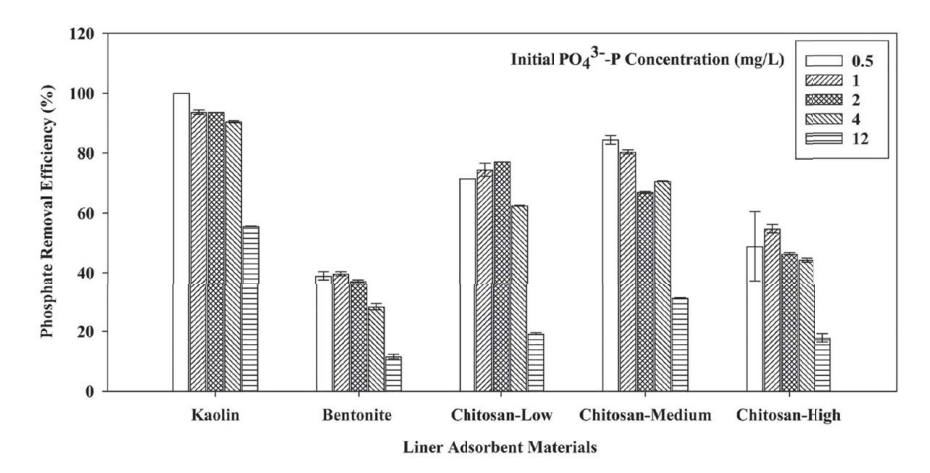


Fig. 3. Phosphate removal by the selected clay and chitosan materials at the selected initial phosphate concentrations.

phosphate concentration was observed for the tested chitosan materials. The ORP ranged from 175.9 to 219.8 mV for the tested phosphate concentrations. EC did not vary significantly with phosphate concentration for any of the tested chitosan materials; however, the EC for the medium-molecular-weight chitosan solutions (0.43–0.65 mS/cm) was higher than that of the solutions from either the low-molecular-weight (0.17–0.22 mS/cm) or high-molecular-weight (0.26–0.32 mS/cm) chitosan materials. The higher EC obtained for filtrate solutions of medium-molecular-weight chitosan may be due to the high degree of deacetylation (87%–88%) associated with medium-molecular-weight chitosan compared to the other two chitosan materials [Fig. 2(c)].

Comparisons between the solutions exposed to the clay materials and solutions exposed to the chitosan materials indicate differences in the final solution properties. These differences between the solution properties of different materials are driven mainly by the properties of the materials such as dissolution reactions in clays and the slightly basic nature of chitosan. The pH of all the filtrate solutions when exposed to bentonite was higher than that of the solutions when exposed to kaolin since the dissolution reactions of minerals in bentonite can result in the reduction of H⁺ ions, as described previously. The solution pH for all solutions exposed to chitosan was higher than the pH of the solutions exposed to kaolin but less than the pH of the solutions exposed to bentonite.

Fig. 4. Possible mechanisms of phosphate removal by (a) ion exchange by metal oxides in clays (adapted from Asomaning 2020); and (b) electrostatic attraction in chitosan.

The solutions exposed to chitosan had lower ORP values than the kaolin solutions and slightly greater ORP values than the bentonite solutions. All tested chitosan solutions had EC values higher than the kaolin solutions but lower than the bentonite solutions, meaning that the supernatants from the kaolin batch tests had the least number of free ions compared to all the other materials, while the bentonite filtrate solutions had the highest number of free ions.

Phosphate Removal

Fig. 3 shows the phosphate removal efficiency of the selected materials at the selected initial phosphate concentrations. The phosphate removal efficiency results are each presented as the average of two values (duplicate tests). Additionally, each clay and chitosan material was subjected to batch tests (duplicates) with deionized water (0 mg/L phosphate) to determine whether any of the tested materials would release or leach phosphate into the aqueous solution. The chemical composition of both bentonite and kaolin includes some phosphorus (Table 2), while the chemical composition of chitosan does not. Kaolin and bentonite released 0.0014 and 0.0037 mg of PO₄³-P per gram of material into the aqueous solution, respectively. No phosphate release was observed for any of the chitosan materials (low, medium, and high molecular weights).

The phosphate removal efficiencies for kaolin and bentonite are shown in Fig. 3. For kaolin, the percentage removal efficiency of phosphate ranged from 90.42% to 100% for phosphate concentrations of 0.5–4.0 mg/L. A significant decrease in removal efficiency (56%) was observed for the highest phosphate concentration (12 mg/L). Bentonite phosphate removal efficiency was significantly less than that of kaolin. The results of the bentonite batch tests showed that the phosphate removal efficiency ranged from 12% to 40%. For bentonite, the higher removal efficiencies were achieved at the lower tested phosphate concentrations (0.5, 1, and 2 mg/L PO_4^{3-} -P), and the lowest removal efficiencies were at tested phosphate concentrations of 4 and 12 mg/L. As the concentration of the phosphate solution increases, the accessibility of active adsorption sites on the surface of the kaolin or bentonite progressively diminishes. At higher concentrations, a greater number of phosphate molecules contend for the fixed quantity of available surface sites on the adsorbent, consequently leading to a decline in the efficiency of phosphate removal.

Several factors influence the adsorption capacity of clay mineral soils, such as kaolin and bentonite, particularly their mineralogical composition. The mechanisms involved in phosphate adsorption by

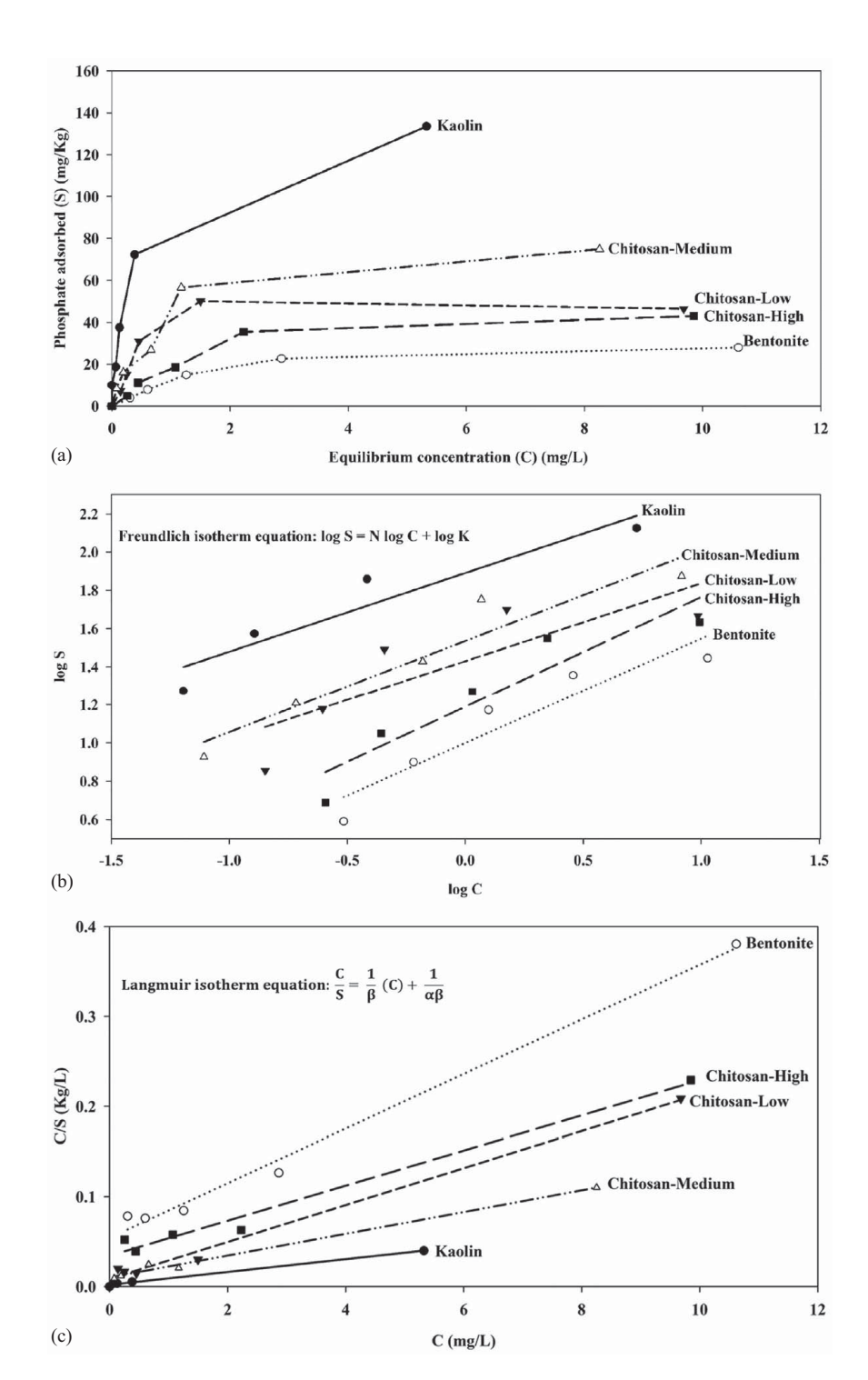


Fig. 5. Phosphate removal by the selected clays and chitosans: (a) batch adsorption test results; (b) Freundlich isotherm model fit; and (c) Langmuir isotherm model fit.

Table 4. Freundlich and Langmuir isotherm model parameters for phosphate adsorption by the clay and chitosan materials used in this study

Materials	Freundlich			Langmuir		
	K (L/kg)	N	R^2	α (L/mg)	β (mg/kg)	R^2
Kaolin	77.79	0.41	0.90	3.55	140.85	1.00
Bentonite	9.99	0.55	0.89	0.56	33.00	0.99
Chitosan-low	26.87	0.41	0.69	2.38	48.78	0.99
Chitosan-medium	34.34	0.48	0.92	1.17	82.64	0.99
Chitosan-high	15.46	0.63	0.87	0.57	51.28	0.98

clay minerals include surface adsorption and precipitation (Fig. 4) (Asomaning 2020; Del Campillo et al. 1999). The presence of amorphous aluminum and iron oxides plays a critical role in determining the adsorption of phosphate. Phosphate reacts with free aluminum and iron ions, resulting in the formation of precipitates, such as AlPO₄, on the surface (Asomaning 2020; Edzwald et al. 1976). The increased efficiency of kaolin over bentonite in removing phosphate may be attributed to the higher concentration of active/free iron and aluminum ions due to the presence of aluminum oxides in the kaolin composition (Table 2) (Coleman 1943). Even though the difference in the amount of aluminum oxide between the two materials is not significant, the slightly acidic pH of kaolin compared to the basic pH of bentonite (Fig. 2) may also be a contributing factor to the higher phosphate removal efficiency of kaolin since preferential dissociation of aluminum ions occurs in acidic environments (Wieland and Stumm 1992; Huang et al. 2009).

Phosphate removal efficiencies of the chitosan materials are shown in Fig. 3. For each tested initial phosphate concentration, the chitosan materials had removal efficiencies greater than bentonite but lower than kaolin. The removal efficiency of low-molecular-weight chitosan was between 77% and 19%. The removal efficiency increased slightly with increasing initial phosphate concentration from 0.5 to 2 mg/L and then decreased with increasing phosphate concentrations of 4 and 12 mg/L. The phosphate removal efficiency of the medium-molecular-weight chitosan ranged from 84% to 31%. The removal efficiency was significantly reduced at the phosphate concentration of 12 mg/L. Batch test results for high-molecular-weight chitosan show that the phosphate removal efficiency ranged from 55% to 18%. The removal efficiency decreased with increasing phosphate concentration, significantly decreasing at a phosphate concentration of 12 mg/L.

The likely mechanism involved in the sorption of phosphate by chitosan is electrostatic attraction between negatively charged PO₄³-P ions and positively charged (protonated) amino groups present on the chitosan molecules (Fig. 4) (Szymczyk et al. 2016). As previously discussed, several factors, including the degree of deacetylation, molecular weight, and source of feedstock, can influence the adsorption capacity of chitosan. It is worth noting that the medium-molecular-weight chitosan, obtained from a mixture of crab and shrimp shells, has a different feedstock source from the low- and high-molecular-weight chitosan derived solely from shrimp shells. This difference in feedstock source and the higher degree of deacetylation (Table 3) likely contributes to the high phosphate removal efficiency observed with medium-molecular-weight chitosan. This contradicts the notion that higher-molecular-weight chitosan necessarily translates to higher removal efficiency. A detailed analysis of the respective properties affecting the adsorption of all three types of chitosan is essential to comprehensively understanding phosphate adsorption behavior. Such an analysis would provide valuable insights into the factors contributing to the variations observed in phosphate removal by these materials. However, this detailed analysis was beyond the scope of this study but will be addressed in future work.

Adsorption Isotherms

The batch sorption test results and the Freundlich and Langmuir adsorption isotherm models of PO_4^{3-} -P removal of the tested materials are presented in Figs. 5(a-c), respectively. The results, as seen in Fig. 5(a), indicate that kaolin exhibits the greatest PO_4^{3-} -P adsorption capacity and that the kaolin maximum adsorption capacity was not reached for the tested phosphate concentration range. This indicates the presence of remaining sites available for adsorption on the kaolin particle surfaces. The results for bentonite,

low-molecular-weight chitosan, and high-molecular-weight chitosan show that these materials have nearly reached their maximum adsorption capacities, signifying that there are relatively fewer available sites for adsorption on the surfaces of these materials at the higher tested phosphate concentrations. However, all three chitosan materials had adsorption capacities greater than bentonite but lower than kaolin. Of the three tested chitosan materials, the medium-molecular-weight chitosan appears to have the greatest PO_4^{3-} -P adsorption capacity.

The parameters of Freundlich and Langmuir isotherm models obtained from Figs. 5(b and c) are listed in Table 4. The results suggest that the Langmuir adsorption isotherm model is the best fit for phosphate adsorption for all the tested materials (as evidenced by the higher R^2 values). According to the Langmuir adsorption model, the maximum adsorption capacities obtained for kaolin, bentonite, low-molecular-weight chitosan, medium-molecular-weight chitosan, and high-molecular-weight chitosan are 140.85, 33, 48.78, 82.64, and 51.28 mg/kg, respectively. However, the maximum adsorption observed in the tested ranges is 133.5, 27.91, 46.38, 74.91, and 42.97 mg/kg for kaolin, bentonite, low-molecular-weight chitosan, medium-molecular-weight chitosan, and high-molecularweight chitosan, respectively. As explained earlier, bentonite, low-molecular-weight chitosan, and high-molecular-weight chitosan have relatively lower adsorption capacities than kaolin and medium-molecular-weight chitosan. The study's results indicate that chitosan when used as a standalone material can assist in the adsorption of phosphate. However, further investigations are necessary to evaluate its effectiveness in combination with other materials, as chitosan's high hydraulic conductivity and biodegradability preclude its use as a liner material alone. Additionally, it is necessary to conduct further experiments with different contaminants and varying chitosan properties to gain a comprehensive understanding of chitosan's usefulness as a constituent of clay composite liners.

Conclusions

This study aims to quantify the phosphate adsorption capacity of five materials: kaolin, bentonite, and low-, medium-, and high-molecular-weight chitosan. Batch experiments are performed with each material individually at different initial phosphate concentrations. The pH, oxidation-reduction potential, electrical conductivity, and phosphate concentration of filtrate solution samples taken at the end of the batch tests are measured. The results of the batch experiments indicate that chitosan has a lower phosphate removal efficiency than kaolin but higher removal efficiency than bentonite. Kaolin exhibits the highest phosphate removal efficiency, ranging from 100% to 56%. The other materials, in decreasing order of efficiency, are medium-molecular-weight chitosan (84% to 31%), low-molecular-weight chitosan (77% to 19%), high-molecular-weight chitosan (55% to 18%), and bentonite (40% to 12%). The Langmuir adsorption isotherm model is the best fit for phosphate adsorption for the selected materials compared to the Freundlich isotherm. The adsorption isotherm results indicate that kaolin did not reach its maximum adsorption capacity for the conditions tested here, whereas bentonite and low- and high-molecular-weight chitosan likely were relatively closer to their maximum adsorption capacity. While the results presented here indicate that chitosan may have the potential for use as a liner material based on its adsorption capabilities, further research is required to investigate other material properties of chitosan relevant to liner materials.

Data Availability Statement

All data, models, and codes generated or used during the study appear in the published article.

Acknowledgments

This research is a part of a comprehensive project titled "Development of Novel Chitosan-Biochar-Bentonite Composite Barrier Resilient to Changing Climate: Synthesis, Characterization, and Containment Mechanisms" funded by the National Science Foundation (CMMI# 2225303), which is gratefully acknowledged. Any opinions, findings, conclusions, and recommendations expressed in this material are those of the authors and do not necessarily reflect the views of the NSF.

References

- Abd El-Hack, M. E., M. T. El-Saadony, M. E. Shafi, N. M. Zabermawi, M. Arif, G. E. Batiha, A. F. Khafaga, Y. M. Abd El-Hakim, and A. A. Al-Sagheer. 2020. "Antimicrobial and antioxidant properties of chitosan and its derivatives and their applications: A review." *Int. J. Biol. Macromol.* 164: 2726–2744. https://doi.org/10.1016/j.ijbiomac.2020.08.153.
- Adhikari, R. A., K. C. Bal Krishna, and R. Sarukkalige. 2016. "Evaluation of phosphorus adsorption capacity of various filter materials from aqueous solution." *Adsorpt. Sci. Technol.* 34 (4–5): 320–330. https://doi.org /10.1177/0263617416653121.
- Alam, M. Z., and A. H. M. Faisal Anwar. 2020. "Nutrients adsorption onto biochar and alum sludge for treating stormwater." *J. Water Environ. Technol.* 18 (2): 132–146. https://doi.org/10.2965/jwet.19-077.
- APHA, AWWA, WEF (American Public Health Association, American Water Works Association and Water Environment Federation). 2005. Standard methods for the examination of water and wastewater, 7–15. 23rd ed. Washington, DC: APHA, AWWA, WEF.
- Asomaning, S. K. 2020. "Processes and factors affecting phosphorus sorption in soils." In Vol. 45 of *Sorption in 2020s*, edited by G. Kyzas and N. Lazaridis, 1–16. Amsterdam, Netherlands: Elsevier.
- ASTM. 2014a. Standard test methods for specific gravity of soil solids by water pycnometer. ASTM D854-14. West Conshohocken, PA: ASTM.
- ASTM. 2014b. Standard test methods for oxidation-reduction potential of water. ASTM D1498. West Conshohocken, PA: ASTM.
- ASTM. 2016. Standard test methods particle-size analysis of soils. ASTM D422. West Conshohocken, PA: ASTM.
- ASTM. 2017. Standard test methods for liquid limit, plastic limit, and plasticity index of soils. ASTM D4318. West Conshohocken, PA: ASTM.
- ASTM. 2018. *Standard test methods for pH of water*. ASTM D1293. West Conshohocken, PA: ASTM.
- ASTM. 2019. Standard test methods for pH of soils. ASTM D4972-19. West Conshohocken, PA: ASTM.
- ASTM. 2023. Standard test methods for electrical conductivity and resistivity of water. ASTM D1125. West Conshohocken, PA: ASTM.
- Cama, J., and J. Ganor. 2015. "Dissolution kinetics of clay minerals." Dev. Clay Sci. 6: 101–153. https://doi.org/10.1016/B978-0-08-100027-4 .00004-8.
- Coleman, R. 1943. "The adsorption of phosphate by kaolinitic and mont-morillonitic clays." Soil Sci. Soc. Am. J. 7 (C): 134–138. https://doi.org/10.2136/sssaj1943.036159950007000C0020x.
- Deka, A., and S. Sekharan. 2017. "Contaminant retention characteristics of fly ash-bentonite mixes." *Waste Manage. Res.* 35 (1): 40–46. https://doi.org/10.1177/0734242X16670002.
- Del Campillo, M. C., S. E. A. T. M. Van der Zee, and J. Torrent. 1999. "Modelling long-term phosphorus leaching and changes in phosphorus fertility in excessively fertilized acid sandy soils." *Eur. J. Soil Sci.* 50 (3): 391–399. https://doi.org/10.1046/j.1365-2389.1999.00244.x.

- Deng, Y. 2020. "Low-cost adsorbents for urban stormwater pollution control." Front. Environ. Sci. Eng. 14: 1–8. https://doi.org/10.1007/s11783-020-1262-9.
- Edzwald, J. K., D. C. Toensing, and M. C.-Y. Leung. 1976. "Phosphate adsorption reactions with clay minerals." *Environ. Sci. Technol.* 10 (5): 485–490. https://doi.org/10.1021/es60116a001.
- Eltaweil, A. S., A. M. Omer, H. G. El-Aqapa, N. M. Gaber, N. F. Attia, G. M. El-Subruiti, M. S. Mohy-Eldin, and E. M. Abd El-Monaem. 2021. "Chitosan based adsorbents for the removal of phosphate and nitrate: A critical review." *Carbohydr. Polym.* 274: 118671. https://doi.org/10.1016/j.carbpol.2021.118671.
- Feng, P., Y. Luo, C. Ke, H. Qiu, W. Wang, Y. Zhu, R. Hou, L. Xu, and S. Wu. 2021. "Chitosan-based functional materials for skin wound repair: Mechanisms and applications." *Front. Bioeng. Biotechnol.* 9: 650598. https://doi.org/10.3389/fbioe.2021.650598.
- Ferrazzo, S. T., R. de Souza Tímbola, L. Bragagnolo, E. Prestes, E. P. Korf, P. D. M. Prietto, and C. Ulsen. 2020. "Effects of acidic attack on chemical, mineralogical, and morphological properties of geomaterials." *Environ. Sci. Pollut. Res.* 27: 37718–37732.
- Gamage, A., and F. Shahidi. 2007. "Use of chitosan for the removal of metal ion contaminants and proteins from water." Food Chem. 104 (3): 989–996. https://doi.org/10.1016/j.foodchem.2007.01.004.
- Guibal, E., M. Van Vooren, B. A. Dempsey, and J. Roussy. 2006. "A review of the use of chitosan for the removal of particulate and dissolved contaminants." Sep. Sci. Technol. 41 (11): 2487–2514. https://doi.org/10.1080/01496390600742807.
- Hance, R. J. 1967. "The speed of attainment of sorption equilibria in some systems involving herbicides." Weed Res. 7 (1): 29–36. https://doi.org /10.1111/j.1365-3180.1967.tb01345.x.
- Harmayani, K. D., and A. H. M. Faisal Anwar. 2016. "Adsorption kinetics and equilibrium study of nitrogen species onto radiata pine (*Pinus radiata*) sawdust." Water Sci. Technol. 74 (2): 402–415. https://doi.org/10.2166/wst.2016.217.
- Holtz, R. D., W. D. Kovacs, and T. C. Sheahan. 2011. An introduction to geotechnical engineering. 2nd ed. Upper Saddle River, NJ: Prentice-Hall.
- Huang, X., G. D. Foster, R. V. Honeychuck, and J. A. Schreifels. 2009. "The maximum of phosphate adsorption at pH 4.0: Why it appears on aluminum oxides but not on iron oxides." *Langmuir* 25 (8): 4450–4461. https://doi.org/10.1021/la803302m.
- Kalam, S., S. A. Abu-Khamsin, M. S. Kamal, and S. Patil. 2021. "Surfactant adsorption isotherms: A review." *ACS Omega* 6 (48): 32342–32348. https://doi.org/10.1021/acsomega.1c04661.
- Kamari, A., I. D. Pulford, and J. S. J. Hargreaves. 2011. "Chitosan as a potential amendment to remediate metal contaminated soil—A characterisation study." *Colloids Surf.*, B 82 (1): 71–80. https://doi.org/10.1016/j.colsurfb.2010.08.019.
- Kaufhold, S., R. Dohrmann, D. Koch, and G. Houben. 2008. "The pH of aqueous bentonite suspensions." Clays Clay Minerals 56 (3): 338–343.
- Lee, J. H., and K. W. Bang. 2000. "Characterization of urban stormwater runoff." Water Res. 34 (6): 1773–1780. https://doi.org/10.1016/S0043 -1354(99)00325-5.
- Li, W., Z. Shen, T. Tian, R. Liu, and J. Qiu. 2012. "Temporal variation of heavy metal pollution in urban stormwater runoff." Front. Environ. Sci. Eng. 6: 692–700.
- Liu, X.-q., X.-x. Zhao, Y. Liu, and T.-a. Zhang. 2022. "Review on preparation and adsorption properties of chitosan and chitosan composites." *Polym. Bull.* 79: 2633–2665. https://doi.org/10.1007/s00289-021-03626-9.
- Ma, J., K. Tracy, and J. Lenhart. 2009. "Phosphorus removal in urban runoff using adsorptive filtration media." In *Proc., StormCon*, 16–20. Blacksburg, VA: Virginia Tech.
- May, D., and M. Sivakumar. 2009. "Prediction of nutrient concentrations in urban storm water." J. Environ. Eng. 135 (8): 586–594. https://doi.org /10.1061/(ASCE)EE.1943-7870.0000027.
- Miretzky, P., and A. F. Cirelli. 2009. "Hg(II) removal from water by chitosan and chitosan derivatives: A review." *J. Hazard. Mater.* 167 (1–3): 10–23. https://doi.org/10.1016/j.jhazmat.2009.01.060.
- Mirzai, M., and S. Asadabadi. 2022. "Magnetic nanocomposites containing low and medium-molecular weight chitosan for dye adsorption: Hydrophilic property versus functional groups." *J. Polym. Environ*. 30: 1560–1573. https://doi.org/10.1007/s10924-021-02300-5.

- OECD (Organisation for Economic Co-operation and Development). 2000. "Adsorption—desorption using a batch equilibrium method." In Vol. 106 of *OECD guideline for testing chemicals*, 1–42. Paris: OECD Publishing.
- Pasek, M. A. 2008. "Rethinking early earth phosphorus geochemistry." PNAS 105 (3): 853–858. https://doi.org/10.1073/pnas.0708205105.
- Pontoni, L., and M. Fabbricino. 2012. "Use of chitosan and chitosan-derivatives to remove arsenic from aqueous solutions—A mini review." *Carbohydr. Res.* 356: 86–92. https://doi.org/10.1016/j.carres.2012.03.042.
- Qin, C., H. Li, Q. Xiao, Y. Liu, J. Zhu, and Y. Du. 2006. "Water-solubility of chitosan and its antimicrobial activity." *Carbohydr. Polym.* 63 (3): 367–374. https://doi.org/10.1016/j.carbpol.2005.09.023.
- Rajeswari, A., A. Amalraj, and A. Pius. 2015. "Removal of phosphate using chitosan-polymer composites." *J. Environ. Chem. Eng.* 3 (4): 2331–2341. https://doi.org/10.1016/j.jece.2015.08.022.
- Reddy, K. R., T. Xie, and S. Dastgheibi. 2014. "Nutrients removal from urban stormwater by different filter materials." *Water Air Soil Pollut*. 225: 1–14. https://doi.org/10.1007/s11270-013-1778-8.
- Sharma, H. D., and K. R. Reddy. 2004. Geoenvironmental engineering: Site remediation, waste containment, and emerging waste management technologies. Hoboken, NJ: Wiley.
- Szymczyk, P., U. Filipkowska, T. Jóźwiak, and M. Kuczajowska-Zadrożna. 2016. "Phosphate removal from aqueous solutions by chitin and chitosan in flakes." Prog. Chem. Appl. Chitin Deriv. 21: 192–202.
- Tolaimate, A., J. Desbrieres, M. Rhazi, A. Alagui, M. Vincendon, and P. Vottero. 2000. "On the influence of deacetylation process on

- the physicochemical characteristics of chitosan from squid chitin." *Polymer* 41 (7): 2463–2469. https://doi.org/10.1016/S0032-3861(99) 00400-0.
- USEPA. 2022a. Climate change indicators: Greenhouse gases. Washington, DC: USEPA.
- USEPA. 2022b. *Understanding global warming potentials*. Washington, DC: USEPA.
- Wan, M. W., I. G. Petrisor, H. T. Lai, D. Kim, and T. F. Yen. 2004. "Copper adsorption through chitosan immobilized on sand to demonstrate the feasibility for in situ soil decontamination." *Carbohydr. Polym.* 55 (3): 249–254. https://doi.org/10.1016/j.carbpol.2003.09.009.
- Wieland, E., and W. Stumm. 1992. "Dissolution kinetics of kaolinite in acidic aqueous solutions at 25°C." Geochim. Cosmochim. Acta 56: 3339–3355. https://doi.org/10.1016/0016-7037(92)90382-S.
- Yaghoobi-Rahni, S., B. Rezaei, and N. Mirghaffari. 2017. "Bentonite surface modification and characterization for high selective phosphate adsorption from aqueous media and its application for wastewater treatments." J. Water Reuse Desalin. 7 (2): 175–186. https://doi.org/10.2166/wrd.2016.212.
- Yang, R., H. Li, M. Huang, H. Yang, and A. Li. 2016. "A review on chitosan-based flocculants and their applications in water treatment." Water Res. 95: 59–89.
- Zhou, A., H. Tang, and D. Wang. 2005. "Phosphorus adsorption on natural sediments: Modeling and effects of pH and sediment composition." *Water Res.* 39 (7): 1245–1254. https://doi.org/10.1016/j.watres.2005 01 026